Author(s): Cunliffe, M; Whiteley, AS; Newbold, L; Oliver, A; Schafer, H; Murrell, JC

Article Title: Comparison of Bacterioneuston and Bacterioplankton Dynamics during a Phytoplankton Bloom in a Fjord Mesocosm

Year of publication: 2009

Link to published version:
http://dx.doi.org/ 10.1128/AEM.01374-09
Publisher statement: None

AEM Accepts, published online ahead of print on 25 September 2009
Appl. Environ. Microbiol. doi:10.1128/AEM.01374-09

Comparison of bacterioneuston and bacterioplankton dynamics during a phytoplankton bloom in a fjord mesocosm

Michael Cunliffe[1], Andrew S. Whiteley[2], Lindsay Newbold[2], Anna Oliver[2], Hendrik Schäfer[3] & J. Colin Murrell[1]*

[1]Department of Biological Sciences, University of Warwick, Gibbet Hill Road, Coventry, CV4 7AL, UK.

[2] Centre for Ecology and Hydrology, Mansfield Road, Oxford, OX1 3SR, UK.

[3] Warwick HRI, University of Warwick, Wellesbourne, CV35 9EF, UK.

*For correspondence. E: j.c.murrell@warwick.ac.uk
T: (+44) 24 7652 3553
F: (+44) 24 7652 3568

ABSTRACT

The bacterioneuston is the community of *Bacteria* present in surface microlayers, the thin surface film that forms the interface between aquatic environments and the atmosphere. In this study we compared bacterial cell abundance and bacterial community structure of the bacterioneuston and the bacterioplankton (from the subsurface water column) during a phytoplankton bloom mesocosm experiment. Bacterial cell abundance, determined by flow cytometry, followed a typical bacterioplankton response to a phytoplankton bloom, with *Synechococcus* and high nucleic acid (HNA) bacterial cell numbers initially falling, probably due to selective protist grazing. Subsequently HNA and low nucleic acid (LNA) bacterial cells increased in abundance but *Synechococcus* did not. There was no significant difference between bacterioneuston and bacterioplankton cell abundances during the experiment. Conversely, distinct and consistent differences between the bacterioneuston and the bacterioplankton community structure were observed. This was monitored simultaneously by *Bacteria* 16S rRNA gene terminal restriction fragment length polymorphism (T-RFLP) and denaturing gradient gel electrophoresis (DGGE). The conserved patterns of community structure observed in all of the mesocosms indicate that the bacterioneuston is distinctive and non-random.

INTRODUCTION

Determining and understanding both spatial and temporal patterns in bacterioplankton community structure is a core aim of marine microbial ecology (15). Distributions of bacterioplankton over space and time can be correlated to environmental parameters and subsequent links can therefore be made to ecosystem function. A broad range of spatial studies made on macro- (34), meso- (20) and micro- (27) scales have shown clear patterns in distribution of the bacterioplankton.

The sea surface microlayer is part of the air-sea interface and is generally considered to be the top 1 mm or less of the ocean (26). Surface microlayers have a fundamental role in regulating transport processes between the ocean and the atmosphere (26) and are often referred to as the neuston (28, 31). For over 25 years it has been hypothesised that the sea surface microlayer is a hydrated gelatinous layer (40) that contains surface active organic compounds such as carbohydrates, proteins, lipids and humic substances, in relatively high concentrations (17, 45, 48). Recently, gel-like transparent expolymer particles (TEP) have been shown to be enriched in the surface microlayer, supporting the concept of a gelatinous interfacial layer (46).

Bacteria present in surface microlayers or the neuston are regarded as the bacterioneuston. There are relatively few studies which have directly compared the community structure of the bacterioneuston with that of the cognate subsurface (bacterioplankton) in the marine environment. Analysis of *Bacteria* 16S rRNA gene clone libraries constructed using DNA isolated from surface microlayer and subsurface water (<1 m) samples from the North Sea revealed that the bacterioneuston was dominated by two operational taxonomic units which accounted for 81% of clones analysed (13). Community structure profiling using denaturing gradient gel electrophoresis (DGGE) of the bacterioneuston at three sites around Oahu Island in

64 the Pacific Ocean showed that the bacterioneuston forms consistent and distinct
65 community structures. Conversely, *Archaea* community structure of the same samples
66 using *Archaea* 16S rRNA gene DGGE analysis did not show the same surface
67 microlayer-specific response, indicating that *Bacteria* and *Archaea* respond to their
68 environment in fundamentally different ways in the neuston (7).

69 Other studies, have however, reported no consistent differences between the
70 bacterioneuston and the bacterioplankton. Samples collected from two separate sites
71 in the Mediterranean Sea were analysed using single strand conformation
72 polymorphism (SSCP) of *Bacteria* 16S rRNA genes (1). The authors did not report
73 any significant differences between the surface microlayer and subsurface samples
74 using this community profiling method.

75 Non-marine studies of the bacterioneuston and *Archaea* communities in
76 estuarine (10) and freshwater (5, 19) environments have also shown distinct microbial
77 community structures present in the surface microlayer compared to those in
78 subsurface water ≤ 1 m below.

79 Recurring phytoplankton blooms are a key feature of coastal waters and
80 strongly influence bacterioplankton community structure and succession (4, 14, 38).
81 Phytoplankton blooms stimulate the bacterioplankton by the release of dissolved
82 organic matter (22) or affect bacterioplankton negatively by direct competition for
83 resources (6). Bacterioplankton community structure may also be influenced by
84 grazing flagellates or viral lysis (47).

85 Mesocosm experiments have been used to study plankton ecology for many
86 decades (33). Mesocosms facilitate study of the effects of key environmental
87 parameters, such as temperature, on plankton communities and allow the succession
88 of natural plankton communities that resemble those found in the marine environment

89 (11). The enclosed water mass means that experiments can be designed which
90 manipulate physicochemical parameters to observe biological effects. Furthermore,
91 with replicated mesocosms, the data collected can be analysed with statistics
92 rigorously. In this study we monitored the dynamics of the bacterioneuston and the
93 bacterioplankton in mesocosms of fjord surface water during an artificially induced
94 phytoplankton bloom, comparing bacterial abundance and bacterial community
95 structure in the surface microlayer and subsurface water.
96

MATERIALS AND METHODS

Mesocosm set-up and sampling

The experiment was carried out at the Marine Biological Field Station, Espeland, Norway (20 km south of Bergen) from 21 May 2008 - 1 June 2008. Twelve land-based mesocosms (1.5 m diameter and 1.5 m deep) were each filled (2,474 L) with pre-filtered (~300 µm) water from the Raunefjorden. The water in the mesocosms was kept mixed with submerged aquarium pumps. The mesocosms were contained in three larger open containers (Figure 1A) that were filled and circulated constantly with pumped fjord water to maintain the mesocosms at ambient fjord temperature. The twelve mesocosms were divided into two treatment groups, control and nutrient amended, allowing six replicate mesocosms for each treatment. Each of the larger containers held two control mesocosms and two nutrient amended mesocosms (Figure 1B). Addition of nitrate and phosphate according to the Redfield stoichiometry (N:P = 16:1) (35), as 16µM $NaNO_3$ and 1µM KH_2PO_4,was used to induce the phytoplankton bloom at 21.00 hours on day zero.

Sampling took place every day for eleven days at 09.00 hours. Subsurface waters were sampled from a depth of 0.75 m in the centre of the mesocosms using a siphon. The surface microlayer was sampled using two different methods, a mesh screen (Garrett screen) and polycarbonate membranes taken from the centre of the mesocosms. The methods sample two different depths, the mesh screen removes the top ~400 µm and the polycarbonate membrane removes the top ~40 µm of the surface microlayer (7). The mesh screen (16-mesh stainless steel screen: size 275 × 275 mm) was placed below the surface water, lifted horizontally through the surface microlayer and the water was collected into a sterile bottle. 250 mL was then filtered using a peristaltic pump through a Sterivex™-GS filter unit (pore size 0.2 µm; Millipore).

After all the water had been evacuated from the filter unit, 1.6 mL RNAlater® (Ambion) was added and the filter unit was stored at 4°C. Polycarbonate membranes (47 mm diameter; pore size 0.2 µm; ISOPORE™; Millipore) were placed onto the water surface using forceps and left for 10 sec before being removed and stored in 2 mL screw cap tubes at -20°C.

Dissolved inorganic nutrients

Subsurface water samples were filtered (Sterivex™-GS; pore size 0.2 µm; Millipore) before being stored in polyethylene vials at -20°C until nitrate, nitrite, phosphate and silicate were determined using standard segmented flow analysis with photometric procedures (18).

Phytoplankton and bacterial cell counts

Phytoplankton and bacterial cells in the mesocosms were enumerated with a Becton Dickinson FACScalibur benchtop flow cytometer (BD Bioscience) equipped with a 488 nm laser line. Cells were enumerated in samples collected from the subsurface and mesh screens only, since membrane collected samples do not remove enough water for flow cytometry analysis. Two analyses were performed per sample to determine both phytoplankton and bacterial cell counts. Briefly, phytoplankton (picoeukaryotes, coccolithophorids, small and large nanoplankton) and *Synechococcus* cell counts were enumerated on fresh unstained samples using modified flow rates (ca. 100 µL min^{-1}) and pre- and post- aspiration sample weighing together with timed acquisition (5 min) (42). Bacterial cell counts (total count and sub-sets for high nucleic acid (HNA) and low nucleic acid (LNA) bacterial cells) were determined on paraformaldehyde fixed/citrate treated samples stained with SYBR®

147 Green I (Invitrogen) using timed acquisition (2 min) in concert with pre- and post-
148 aspiration weighing (50). For pre- and post-aspiration weighing, all samples were
149 weighed before and after analysis to determine sample volumes aspirated during the
150 sample analysis and internal 0.49 µm reference beads were used to account for flow
151 and machine drift. All analysed samples were exported as listmode files and analysed
152 using Cyflogic to gate major populations and calculate absolute cell concentrations
153 from aspirated volumes.
154
155 **Extraction of DNA for bacterial community structure analysis**
156 DNA was extracted from subsurface, mesh screen and membrane samples collected
157 on day two, day five and day ten. DNA was extracted from three control mesocosms
158 (replicates A, E and K) and three nutrient amended mesocosms (replicates B, F and L)
159 (Figure 1B). DNA was extracted in a sucrose buffer using lysozyme, proteinase K,
160 SDS and phenol-chloroform as described by Cunliffe *et al* (2008). The resuspended
161 DNA was quantified using a spectrophotometer (ND-1000; NanoDrop™) before all
162 DNA samples were diluted to a concentration of 30 ng.μl^{-1} and stored at -20ºC.
163
164 **Bacterial community structure analysis**
165 PCR amplification of *Bacteria* 16S rRNA genes for T-RFLP analysis was performed
166 using a fluorescently labelled primer (6FAM)27F (5′-AGA GTT TGA TCM TGG
167 CTC AG-3′) and primer 536R (5′-GWA TTA CCG CGG CKG CTG-3′) (41). For
168 PCR, a total volume of 50 µl contained 0.5mM dNTPs, 0.5 µM of each primer, 2 units
169 of *Taq* DNA polymerase (Sigma) and 30 ng template DNA. The PCR programme
170 consisted of initial denaturation at 94°C for 2 min followed by 30 cycles of 94°C for 1
171 min, annealing temperature 52°C for 1 min and elongation at 72°C for 3 min and then

a final elongation step at 72°C for 10 min. PCR products were verified by agarose gel electrophoresis and stored at -20ºC.

PCR products were purified using QIAquick PCR Purification Kit (Qiagen) according to the manufacturer's instructions. 20 µl of purified PCR product was digested for 4 hr at 37ºC using the restriction enzyme MspI (Promega). 0.5 µl of the digestion product was combined with denatured 0.5 µl LIZ600 size standard (Applied Biosystems) and formamide before being run on a 3730 DNA sequencer (Applied Biosystems). The sizes of the restriction fragments (T-RFs) were calculated and binned using Genemarker™ (Softgenetics®). Bin widths were checked and manually adjusted to encompass all concordant peaks. To differentiate signal from background, a fluorescence unit threshold of 40 units was used to determine which T-RFs to include. Relative abundance was calculated for each T-RF by dividing individual T-RF fluorescence by total sample fluorescence.

PCR amplification of 16S rRNA genes from *Bacteria* for DGGE analysis was performed using primers 341F (5′- CCT ACG GGA GGC AGC AG -3′) and primer 518R (5′- ATT ACC GCG GCT GCT GG -3′) (30). The same PCR was set up as before for T-RFLP but using the different primers. The PCR programme for DGGE consisted of an initial denaturation at 94°C for 5 min, followed by 35 cycles of 95°C for 1 min, annealing temperature 65-55°C for 20 cycles (reduction of -0.5°C per cycle) and 55°C for 15 cycles, elongation at 72°C for 1 min and then a final elongation step at 72°C for 10 min.

DGGE was performed with a DCode™ system (Biorad). Gels were prepared with 10% (v/v) acrylamide/bisacrylamide with a 30-70% linear denaturant gradient (100% denaturant solution contains 6.9M urea and 11.5M formamide). The gel was run in 1 × TAE buffer at 60˚C for a total of 1,008 Volt hours (constant voltage 63 V,

16 hr). Gels were stained with SYBR® Gold nucleic acid stain (Invitrogen) before the image was captured on a UV trans-illuminator (Syngene).

DGGE bands that were relatively more abundant in the surface microlayer samples were selected and excised. The excised bands were washed in sterile molecular grade water (MGW) before being crushed in 20 µl MGW and incubated at 4ºC for 2hr. The eluted DNA was used to re-amplify the DGGE band using the same PCR primers and conditions as before. DGGE band DNA sequences were obtained using the University of Warwick Molecular Biology Services Laboratory and are available in GenBank (accession numbers GQ902042 to GQ902046).

Statistical and ordination analysis

Analysis of variance (ANOVA) was used to identify statistical significance in the phytoplankton and bacterial cell count data ($n = 6$; $p < 0.05$). Where significant differences were seen, a Tukey's test was used to compare data within a defined set. Both ANOVA and Tukey's test were performed using SPSS statistical software (SPSS). Principal component analysis (PCA) was used to visualise the relationships between bacterial community structures from the T-RFLP data and was carried out using MINITAB® statistical software (Minitab). PCA is used to reduce the complexity of multivariant data (T-RF relative abundance) by producing new variables that account for most of the variation in the original data (39). DGGE profiles of 16S rRNA genes from *Bacteria* were compared using GelCompare®II (Applied Maths) by calculating similarity coefficients using a curve based Pearson correlation, followed by the construction of Unweighted Pair Group Method with Arithmetic mean (UPGMA) dendrograms from the calculated similarity coefficients.

RESULTS

Phytoplankton abundance

The phytoplankton bloom succession in the mesocosms progressed generally as expected based on previous experience from earlier experiments with water collected from Raunefjorden (6, 29). The nitrate and phosphate added to the nutrient amended mesocosms was steadily depleted and levels returned to background concentrations by day nine (Figure 2). The concentration of silicate remained constant throughout the experiment. Nitrite increased in the nutrient amended mesocosms to 0.19 ± 0.01 µM at day five before returning to background levels by day ten (Figure 2).

Phytoplankton cells were divided into four groups by flow cytometry analysis: picoeukaryotes, large nanoplankton, small nanoplankton and coccolithophorids (see Materials and Methods). Picoeukaryote numbers increased in both control and nutrient amended mesocosms at the start of the experiment (Figure 3). By day five a significant increase in picoeukaryote numbers was detected in the nutrient amended mesocosms compared to control mesocosms. The artificially induced picoeukaryote bloom peaked on day seven with a median cell density of ~ 2×10^5 cells.mL^{-1}. There was no detectable significant difference between picoeukaryote cell counts in the surface microlayer compared to their cognate subsurface water samples.

Phytoplankton cells designated as large nanoplankton showed a significant increase in numbers in the nutrient amended mesocosms from day five onwards (Figure 3). As with picoeukaryotes, there was no significant difference between numbers in the surface microlayer and subsurface water.

Small nanoplankton showed more variable cell counts during the time of the experiment compared to picoeukaryotes and large nanoplankton (Figure 3). After day six, a significant difference was detected between the counts in the nutrient amended

mesocosms compared to cell counts in control mesocosms. The bloom of small nanoplankton peaked on day seven before returning to similar cell numbers as the control mesocosms by day nine.

As with the small nanoplankton, coccolithophorid abundance appeared stochastic in contrast to the picoeukaryotes and large nanoplankton cell counts and had no distinct trend. The intra-variation between mesocosms was high for coccolithophorid counts and this subsequently affected statistical analysis. At day seven there was a significant difference between cell counts in the subsurface samples from the control and nutrient amended mesocosms. For the remainder of the experiment the coccolithophorid counts were significantly higher in the nutrient amended mesocosms. There was also some indication of weak enrichment of coccolithophorids in the surface microlayer (Figure 3).

Bacterial abundance

Flow cytometry was used to separate three bacterial cell groups: HNA bacterial cells, LNA bacterial cells and *Synechococcus* cells. The dynamics of the three groups was different during the experiment (Figure 3).

HNA bacterial cells showed a marked decrease in abundance at the start of the experiment with the rate of decrease accelerating rapidly on day three. On day five the HNA bacterial cells numbers had dropped from an initial ~ 6×10^5 cells.mL^{-1} to ~ 1×10^5 cells.mL^{-1}. After day five the abundance of HNA bacterial cells began to increase in all mesocosms and a significant difference between HNA bacterial cell counts in the nutrient amended mesocosms compared to the control mesocosms for the remainder of the experiment was detected (Figure 3). At the end of the experiment HNA bacterial cell numbers reached similar levels to those at the start of the

experiment. There was no significant difference in HNA bacterial cell abundance between surface microlayer and subsurface water samples.

Unlike the HNA bacterial cells, LNA bacterial cells did not show a drastic drop in abundance (Figure 3). LNA bacterial cell abundance fluctuated from day zero to day eight with no overall pattern. At day two and day three there was a significant difference between subsurface and surface microlayer LNA bacterial cell abundance, with less cells in the surface microlayer sample. LNA bacterial cell abundance fluctuated until day nine when there was a significant increase in the nutrient amended mesocosms, peaking at ~ 7×10^5 cells.mL^{-1}.

As with the HNA bacterial cells, *Synechococcus* cell abundance declined at two rates at the start of the experiment. Initially cell abundance dropped slowly up to day three and then rapidly down to ~ 4×10^3 cells.mL^{-1} on day six (Figure 3). Unlike HNA bacterial cells, *Synechococcus* cell abundance did not recover and remained low for the remainder of the experiment. There were no significant differences in abundance of *Synechococcus* between treatments or between surface microlayer and subsurface water.

Bacterial community structure

We used two *Bacteria* 16S rRNA gene profiling methods (T-RFLP and DGGE) to monitor changes in the bacterial community structures in surface microlayer and subsurface water samples collected on day two, day five and day ten.

PCA ordination of the structures of the bacterial communities from T-RFLP analysis of subsurface and surface microlayer DNA samples is shown in Figure 4. On day two, the samples collected from the subsurface and from the surface microlayer using the mesh screen clustered closely together relative to the surface microlayer

297 samples collected using polycarbonate membranes. As the mesocosm blooms
298 progressed, this pattern changed drastically. At day five, samples from the subsurface
299 showed a distinct cluster that was separate from the mesh screen samples. As with day
300 two, the membrane collected surface microlayer samples remain distinct from the
301 subsurface samples. Near the end of the experiment on day ten, bacterial community
302 structure in the samples collected with the mesh screen clustered with the samples
303 collected with membranes and not subsurface water samples. Ordinance analysis of
304 the T-RFLP data in this experiment showed no evidence of bacterial community
305 structural differences as a result of the induced phytoplankton bloom (Figure 4).
306 DGGE analysis of the bacterial community structures showed similar results
307 to the T-RFLP analysis. At day two, subsurface and mesh screen-collected samples
308 were similar and membrane-collected samples showed some differences (Figure 5).
309 This was less pronounced with DGGE than with T-RFLP at day 2. By day five, the
310 membrane collected-samples were distinctly different compared to mesh screen and
311 subsurface samples, forming a separate clade in the dendrogram. Also at day five,
312 some mesh screen collected-samples were different to their associated subsurface
313 samples. By day ten, both the membrane- and mesh screen collected-samples were
314 distinctly different from the subsurface samples, corroborating the results from the T-
315 RFLP analysis. As with the T-RFLP analysis, DGGE analysis confirmed that the
316 bacterial community structures were not affected by the phytoplankton bloom.
317 Five relatively dominant DGGE bands from the surface microlayer samples
318 were excised and sequenced (Figure 5). All five DGGE band DNA sequences were
319 very similar (≥ 98%) to 16S rRNA gene sequences from isolated bacterial strains
320 (Table 1). DGGE bands 1 and 2 were identical to the 16S rRNA gene sequence of
321 *Dokdonia donghaensis* PRO95 (FJ627052) and *Krokinobacter genikus* Cos-13

322 (AB198086) respectively, from the Flavobacteria family Flavobacteriaceae. DGGE

323 DNA sequences 3, 4 and 5 were almost identical to two genera, *Alteromonas* and

324 *Glaciecola* of the Alteromonadaceae (Table 1).

DISCUSSION

Bacterial abundance

Results show that the three bacterial cell types quantified in the mesocosms responded in three different ways (Figure 3). Both HNA bacterial cells and *Synechococcus* cells decreased in numbers drastically at the start of the experiment. HNA bacterial cells and LNA bacterial cells then increased in numbers in the phytoplankton bloom.

An abrupt decrease, followed by an increase in bacterioplankton cell abundance is a characteristic response frequently observed during phytoplankton blooms (4, 6, 29, 36). A previous *Emiliania huxleyi*-dominated mesocosm experiment using Raunefjorden fjord water showed a very similar bacterial cell response (6). Other mesososm experiments at Raunefjorden also reported the same reduction in *Synechococcus* cell abundance during an induced bloom (29), thus indicating that *Synechococcus* are not successful under these conditions and/or are out-competed.

One of the principal sources of bacterial mortality in the water column is protist predation, with many protists grazing selectively (32). Significantly, some protists target rapidly growing and dividing bacterial cells, such as those with HNA content (16, 44). Furthermore, recent evidence suggests that the concomitant drop in bacterial numbers and bloom of small phytoplankton may be due to mixotrophic growth of phytoplankton (49). This may therefore account for the mortality of HNA bacterial cells and *Synechococcus* cells, whereas the LNA bacterial cells did not appear to be affected (Figure 3).

In this study, cell numbers in the bacterioneuston and the bacterioplankton were not significantly different, indicating that there was no enrichment of cells in the surface microlayer. Surface microlayer and subsurface water samples collected from two sites in the Mediterranean Sea also showed that the numbers of *Synechococcus* in

350 the surface microlayer were the same as those in subsurface (0.5 m) samples (23).
351 Bacterial cell counts by flow cytometry analysis from the same samples did have low
352 levels of enrichment in the surface microlayer yet the enrichment of cultivable
353 bacterial cells was much more variable, with enrichment factors ranging from 0.5 to
354 191 (23). High numbers of cultivable bacterial cells in the surface microlayer
355 compared to subsurface waters are often reported (1, 2, 43).
356
357 **Bacterial community structure**
358 Unlike bacterial cell abundance, bacterial community structure was consistently
359 different in the surface microlayer compared to subsurface water. Surface microlayer
360 samples collected using both membranes and a mesh screen showed a reproducibly
361 distinct bacterioneuston in the mesocosms. Previous studies have characterised the
362 marine bacterioneuston and cognate subsurface bacterioplankton in the North Sea
363 (13), the Mediterranean Sea (1) and Pacific Ocean (7). In the North Sea and Pacific
364 Ocean studies the bacterioneuston community structure was distinct compared to that
365 of the bacterioplankton 1 m below the surface (7, 13). Conversely, the Mediterranean
366 Sea study reported no consistent differences between communities (1).
367 The method of surface microlayer sampling is important in the study of the
368 bacterioneuston (7). Even though the sea surface microlayer is considered the top 1
369 mm of the ocean, it is operationally defined by sampling depth (26). We used a mesh
370 screen (sampling depth ~400 µm) and membranes (sampling depth ~ 40 µm) to
371 determine bacterial community structure. Previous comparison of membrane-
372 collected and mesh screen-collected samples from an estuarine surface microlayer
373 showed samples collected using a mesh screen under-represent the bacterioneuston
374 because samples also contain subsurface water, therefore “diluting” the

bacterioneuston sample (7). In this study, at the start of the experiment, the mesh screen-collected bacterial community structures were more similar to the subsurface (bacterioplankton) than to the membrane-collected samples (bacterioneuston). This however changed during the experiment with mesh screen-collected samples becoming more similar to the membrane-collected samples (Figures 4 and 5). This indicated an enrichment effect in the surface microlayer, causing the bacterial communities sampled using the mesh screen to change from bacterioplankton-like to bacterioneuston-like during the experiment.

The proposed enrichment of the surface microlayer and bacterioneuston may be due to the physical nature of the mesososms used in this experiment. Even though the mesocosms were mixed continuously they were calmer than the open fjord. Examination of surface microlayer samples offshore of Barcelona showed, that under calm conditions (low wind speed and cloudless skies) the enrichment of several parameters in the surface microlayer, including heterotrophic *Bacteria* counts, chlorophyll-*a* and suspended particle matter, increasing substantially (23), supporting our observations in the mesocosms.

The methodological approaches used to compare the community structure of the bacterioneuston and the bacterioplankton can also influence data interpretation. Agogue *et al* (2005) used similarity values based upon Jaccard coefficients of SSCP profiles from surface microlayer and subsurface water samples collected in the Mediterranean Sea. Jaccard coefficients are absence/presence based and do not consider relative abundances (21). Franklin *et al* (2005) and Cunliffe *et al* (2009) used 16S rRNA gene clone libraries and DGGE profiles assessed using Pearson correlations, both of which take into account the relative abundances between samples. In this study we also included changes in relative abundances (T-RFs and

DGGE bands). The increased resolution of community structure comparisons made using relative abundances versus comparisons made using absence/presence data may, in part, account for the conclusions of Agogue *et al* (2005).

In this study, bacterial community structure dynamics in each mesocosm were synchronous, showing consistent patterns between replicates (Figures 4 and 5). The bacterioneuston communities at two sites on either side of Oahu Island were more similar to each other than to their cognate subsurface water bacterioplankton communities just 0.4 m below, also indicating non-random assembly of the surface microlayer community (7). Synchronicity of discrete bacterial communities, although poorly understood, is very important, as concordant community dynamics suggests the community structure patterns that emerge are controlled and are not random (24). Therefore, if the bacterioneuston community structure is controlled by the environment and is not random, as our data suggest, then the sea surface microlayer is indeed an important ecological zone of the water column.

Five dominant DGGE bands in the surface microlayer were sequenced and identified (Figure 5 and Table 1). The bands were very similar to just two families, Flavobacteriaceae (Bands 1 and 2) and Alteromonadaceae (Bands 3, 4 and 5). The genera *Alteromonas* and *Glaciecola* (Alteromonadales, Alteromonadaceae) were also prevalent in surface microlayer samples collected from the marine end of Blyth Estuary on the North East Coast of the UK (10). A previous study has also showed the closely related genus *Pseudoalteromonas* (Alteromonadales, Pseudoalteromonadaceae) dominated surface microlayer samples collected from the North Sea, close to the coast of the UK (13).

Bacterial cell abundance compared to community structure

Bacterioplankton in the water column include both free-living and cells attached to several possible surfaces including phytoplankton (25) and marine gels (3). Marine gels are a significant component of the sea surface microlayer, giving it a gelatinous structure (8, 40, 46). Surface microlayer samples collected from the same mesocosms in this study were enriched with transparent exopolymer gel particles (9). Therefore, in the sea surface microlayer more microorganisms maybe attached than free-living (8). Analysis of free-living and attached bacterioplankton communities co-occurring in the water column show that both temporal variability and diversity in the attached community is higher than in the free-living bacterial community (37) and specific attached bacterial communities can develop (12).

The two standard marine microbial ecology approaches used in this study, flow cytometry and community profiling (T-RFLP and DGGE), inherently analyse different components of the free-living and attached bacterial cell pools. We filtered the water samples for DNA extraction and subsequent community profiling, therefore all particles in the water sample > 0.2 µm were analysed by T-RFLP and DGGE, both free-living and attached bacterial cell pools. However, flow cytometry only counts the free-living bacterial cells. This may contribute towards the observations that there are no differences in bacterial cell abundance between the surface microlayer and subsurface water (free-living only), yet there are distinct and consistent differences in the bacterial community structures (free-living and attached). This may also be responsible for the differences reported between flow cytometry bacterial cell counts and bacterial colony forming unit counts in samples collected in the Mediterranean Sea by Joux *et al* (2006).

CONCLUSIONS

The similar dynamics of bacterial cell numbers and community structure between replicate mesocosms described in this study shows how conserved patterns can emerge in bacterial systems such as the sea surface microlayer. These data indicate that the bacterial community structure patterns witnessed in the sea surface microlayer are determined by environmental forces and are not idiosyncratic. This has important implications for marine microbiological research as it is empirical evidence that supports the hypothesis that the surface ocean, particularly the sea surface microlayer, is much more structured than previously thought.

ACKNOWLEDGMENTS

This work was supported by the Natural Environment Research Council (UK) through the project – SOLAS Bergen Mesocosm experiment (NE/E011446/1), which is part of the NERC-Surface Ocean Lower Atmosphere Study (SOLAS) directed programme.

We thank all the people involved in the project who helped with the preparation and sampling of the mesocosms, including Agnes Aadnesen (University of Bergen). We thank Mikal Heldal, Jorun Egge (University of Bergen), Gill Malin (University of East Anglia) and Ian Joint (Plymouth Marine Laboratory) for invaluable advice concerning the set-up and management of mesocosm experiments at Espeland. We also thank Linda Fonnes at the Institute of Marine Research, Bergen, for inorganic nutrient analysis.

REFERENCES

1. **Agogue, H., E. O. Casamayor, M. Bourrain, I. Obernosterer, F. Joux, G. J. Herndl, and P. Lebaron.** 2005. A survey on bacteria inhabiting the sea surface microlayer of coastal ecosystems. FEMS Microbiology Ecology **54:**269-80.
2. **Agogue, H., E. O. Casamayor, F. Joux, I. Obernosterer, C. Dupuy, F. Lantoine, P. Catala, M. G. Weinbauer, T. Reinthaler, G. J. Herndl, and P. Lebaron.** 2004. Comparison of samplers for the biological characterization of the sea surface microlayer. Limnology and Oceanography Methods **2:**213-225.
3. **Alldredge, A. L., U. Passow, and B. E. Logan.** 1993. The abundance and significance of a class of large, transparent organic particles in the ocean. Deep Sea Research Part I **40:**1131-1140.
4. **Allers, E., L. Gomaz-Consarnau, J. Pinhassi, J. M. Gasol, K. Simek, and J. Pernthaler.** 2007. Response of *Alteromonadaceae* and *Rhodobacteriaceae* to glucose and phosphorus manipulation in marine mesocosms. Environ Microbiol **9:**2417-2429.
5. **Auguet, J. C., and E. O. Casamayor.** 2008. A hotspot for cold crenarchaeota in the neuston of high mountain lakes. Environ Microbiol **10:**1080-1086.
6. **Castberg, T., A. Larsen, R. A. Sandaa, C. P. D. Brussaard, J. K. Egge, M. Heldal, R. Thyrhaug, E. J. v. Hannen, and G. Bratbak.** 2001. Microbial population dynamics and diversity during a bloom of the marine coccolithophorid *Emiliania huxleyi* (Haptophyta). Marine Ecology Progress Series **221:**39-46.
7. **Cunliffe, M., E. Harrison, M. Salter, H. Schafer, R. C. Upstill-Goddard, and J. C. Murrell.** 2009. Comparison and validation of sampling strategies

for the molecular microbial ecological analysis of surface microlayers. Aquatic Microbial Ecology **57:**69-77.

8. **Cunliffe, M., and J. C. Murrell.** 2009. The sea surface microlayer is a gelatinous biofilm The ISME Journal **3:**1001–1003.

9. **Cunliffe, M., M. Salter, P. J. Mann, A. S. Whiteley, R. C. Upstill-Goddard, and J. C. Murrell.** 2009. Dissolved organic carbon and bacterial populations in the gelatinous surface microlayer of a Norwegian fjord mesocosm. FEMS Microbiology Letters **299:**248-254.

10. **Cunliffe, M., H. Schafer, E. Harrison, S. Cleave, R. C. Upstill-Goddard, and J. C. Murrell.** 2008. Phylogenetic and functional gene analysis of the bacterial and archaeal communities associated with the surface microlayer of an estuary. The ISME Journal **2:**776-789.

11. **Davis, C. O.** 1982. The importance of understanding phytoplankton life strategies in the design of enclosure experiments p. 323-332. *In* G. D. Grice and M. R. Reeve (ed.), Marine Mesocosms Biological and Chemical Research in Experimental Ecosystems. Springer-Verlag, New York.

12. **DeLong, E. F., D. G. Franks, and A. L. Alldredge.** 1993. Phylogenetic diversity of aggregate-attached vs. free-living marine bacterial assemblages. Limnology and Oceanography **38:**924-934.

13. **Franklin, M. P., I. R. McDonald, D. G. Bourne, N. J. Owens, R. C. Upstill-Goddard, and J. C. Murrell.** 2005. Bacterial diversity in the bacterioneuston (sea surface microlayer): the bacterioneuston through the looking glass. Environ Microbiol **7:**723-36.

14. **Fuhrman, J. A., I. Hewson, M. S. Schwalbach, M. S. Steele, J. A. Brown, and S. Naeem.** 2006. Annually reoccurring bacterial communities are predictable from ocean conditions Proc Natl Acad Sci **103:**13104-13109.

15. **Fuhrman, J. A., and J. A. Steele.** 2008. Community structure of marine bacterioplankton: patterns, networks, and relationships to function. Aquatic Microbial Ecology **53:**69-81.

16. **Gasol, J. M., U. L. Zweifel, F. Peters, J. A. Furhman, and A. Hagstrom.** 1999. Significance of size and nucleic acid content heterogeneity as measured by flow cytometry in natural planktonic bacteria. Appl Environ Microbiol **65:**4475-4483.

17. **Gasparovic, B., Z. Kozarac, A. Saliot, B. Cosovi, and D. Mobius.** 1998. Physicochemical characterization of natural and ex-situ reconstructed sea-surface microlayers. J Colloid Interface Sci **208:**191-202.

18. **Grasshoff, K., K. Kremling, M. Ehrhardt, and L. G. Anderson.** 1999. Methods of seawater analysis. Wiley-VCH, Weinheim.

19. **Hervas, A., and E. O. Casamayor.** 2008. High similarity between bacterioneuston and airborne bacterial community compositions in a high mountain lake area FEMS Microbial Ecology **67:**219-228.

20. **Hewson, I., J. A. Steele, D. G. Capone, and J. A. Furhman.** 2006. Temporal and spatial scales of variation in bacterioplankton assemblages of oligotrophic waters. Marine Ecology Progress Series **311:**67-77.

21. **Jaccard, P.** 1908. Nouvelles recherches sur la distribution florale. Bull Soc Vaudoise Sci Nat **44:**223-270.

22. **Jensen, L. M.** 1983. Phytoplankton release of extracellular organic carbon, molecular weight composition and bacterial assimilation. Marine Ecology Progress Series **11:**39-48.

23. **Joux, F., H. Agogue, I. Obernosterer, C. Dupuy, T. Reinthaler, G. J. Herndl, and P. Lebaron.** 2006. Microbial community structure in the sea surface microlayer at two contrasting coastal sites in the northwestern Mediterranean Sea. Aquatic Microbial Ecology **42:**91-104.

24. **Kent, A. D., A. C. Yannarell, J. A. Rusak, E. W. Triplett, and K. D. McMahon.** 2007. Synchrony in aquatic microbial community dynamics. ISME Journal **1:**38–47.

25. **Kogure, K., U. Simidu, and N. Taga.** 1981. Bacterial attachment to phytoplankton in sea water. Journal of Experimental Marine Biology and Ecology **56:**197-204.

26. **Liss, P. S., and R. A. Duce.** 2005. The sea surface and global change. Cambridge University Press, UK.

27. **Long, R. A., and F. Azam.** 2001. Microscale patchiness of bacterioplankton assemblage richness in seawater. Aquatic Microbial Ecology **26:**103-113.

28. **Marshall, H. G., and L. Burchardt.** 2005. Neuston: Its definition with a historical review regarding its concept and community structure. Archiv Fur Hydrobiologie **164:**429-448.

29. **Martinez-Martinez, J., S. Norland, T. F. Thingstad, D. C. Schroeder, G. Bratbak, W. H. Wilson, and A. Larsen.** 2006. Variability in microbial population dynamics between similarly perturbed mesocosms. Journal of Plankton Research **28:**1-9.

30. **Muyzer, G., E. C. de Waal, and A. G. Uitterlinden.** 1993. Profiling of complex microbial populations by denaturing gradient gel electrophoresis analysis of polymerase chain reaction-amplified genes coding for 16S rRNA. Appl Environ Microbiol **59:**695-700.

31. **Naumann, E.** 1917. Beiträge zur kenntnis des teichnanoplanktons. II. Über das neuston des süßwasser. Biol Zentbl **37:**98-106.

32. **Pernthaler, J.** 2005. Predation on prokaryotes in the water column and its ecological implications. Nature Reviews Microbiology **3:**537-546.

33. **Pettersson, H., F. Gross, and F. Koczy.** 1939. Large-scale plankton culture. Nature **144:**332-333.

34. **Pommier, T., B. Canback, L. Riemann, K. H. Bostrom, K. Simu, P. Lunberg, A. Tunlid, and Å. Hagstrom.** 2007. Global patterns of diversity and community structure in marine bacterioplankton. Molecular Ecology **16:**867–880

35. **Redfield, A. C.** 1934. On the proportions of organic derivations in sea water and their relation to the composition of plankton, p. 177-192. *In* R. J. Daniel (ed.), James Johnstone Memorial Volume. University Press of Liverpool.

36. **Riemann, L., G. F. Steward, and F. Azam.** 2000. Dynamics of bacterial community compostion and activity during a mesocosm diatom bloom. Appl Environ Microbiol **66:**578-587.

37. **Rooney-Varga, J. N., M. W. Giewat, M. C. Savin, S. Sood, M. LeGresley, and J. L. Martin.** 2005. Links between phytoplankton and bacterial community dynamics in a coastal marine environment. Microbial Ecology **49:**163-175.

590 38. **Sapp, M., A. Wichels, K. H. Wiltshire, and G. Gerdts.** 2007. Bacterial
591 community dynamics during the winter-spring transition in the North Sea.
592 FEMS Microbial Ecology **59:**622-637.
593 39. **Shaw, P. J. A.** 2003. Multivariate statistics for the environmental sciences.
594 Arnold, London.
595 40. **Sieburth, J. M.** 1983. Microbiological and organic-chemical processes in the
596 surface and mixed layers, p. 121-172. *In* P. S. Liss and W. G. N. Slinn (ed.),
597 Air-Sea Exchange of Gases and Particles. Reidel Publishers Co, Hingham,
598 MA.
599 41. **Suzuki, M., M. S. Rappe, and S. J. Giovannoni.** 1998. Kinetic basis in
600 estimates of coastal picoplankton community structure obtained by
601 measurements of small-subunit rRNA gene PCR amplicon length
602 heterogeneity. Appl Environ Microbiol **64:**4522-4529.
603 42. **Tarran, G. A., J. L. Heywood, and M. V. Zubkov.** 2006. Latitudinal
604 changes in the standing stock of nano- and picoeukaryotic phytoplankton in
605 the Atlantic Ocean. Deep Sea Research Part II: Topical Studies in
606 Oceanography **53:**1516-1529.
607 43. **Tsyban, A. V.** 1971. Marine bacterioneuston. Journal of Oceanographic
608 Society of Japan **27:**56-66.
609 44. **Vaque, D., E. O. Casamayor, and J. M. Gasol.** 2001. Dynamics of whole
610 community bacterial production and grazing losses in seawater incubations as
611 related to the changes in the proportions of bacteria with different DNA
612 content. Aquatic Microbial Ecology **25:**163-177.
613 45. **Williams, P. M., A. F. Carlucci, S. M. Henrichs, E. S. Vanvleet, S. G.**
614 **Horrigan, F. M. H. Reid, and K. J. Robertson.** 1986. Chemical and

microbiological studies of sea-surface films in the southern gulf of California and off the west-coast of Baja-California. Marine Chemistry **19:**17-98.

46. **Wurl, O., and M. Holmes.** 2008. The gelatinous nature of the sea-surface microlayer. Marine Chemistry **110:**89-97.

47. **Zhang, R., M. Weinbauer, and P. Qian.** 2007. Viruses and flagellates sustain apparent richness and reduce biomass accumulation of bacterioplankton in coastal marine waters. Environ Microbiol **9:**3008-3018.

48. **Zhengbin, Z., L. Liansheng, W. Zhijian, L. Jun, and D. Haibing.** 1998. Physicochemical studies of the sea surface microlayer. J Colloid Interface Sci **204:**294-9.

49. **Zubkov, M. V., and G. A. Tarran.** 2008. High bacterivory by the smallest phytoplankton in the North Atlantic Ocean. Nature **455:**224-226.

50. **Zubkov, M. V., G. A. Tarran, I. Mary, and B. M. Fuchs.** 2008. Differential microbial uptake of dissolved amino acids and amino sugars in surface waters of the Atlantic Ocean. Journal of Plankton Research **30:**211-220.

Table 1. Sequence similarities of excised 16S rRNA gene DGGE bands in Figure 5.

Band	BLAST Match	% similarity (no. of bases)	Taxanomic grouping
1	*Dokdonia donghaensis* PRO95 (FJ627052)	100 (158)	Flavobacteria, Flavobacteriales, Flavobacteriaceae
2	*Krokinobacter genikus* Cos-13 (AB198086)	100 (158)	Flavobacteria, Flavobacteriales, Flavobacteriaceae
3	*Alteromonas* sp. BCw006 (FJ889589)	100 (163)	Gammaproteobacteria, Alteromonadales, Alteromonadaceae
4	*Alteromonas* sp. Oct07-MA-2BB-3 (GQ215064)	100 (163)	Gammaproteobacteria, Alteromonadales, Alteromonadaceae
5	*Glaciecola nitratireducens* FR1064 (AY787042)	98 (161)	Gammaproteobacteria, Alteromonadales, Alteromonadaceae

FIGURE LEGENDS

Figure 1. (A) Photograph showing the mesocosms used in this study. Twelve mesocosms were divided into three larger containers. (B) Each mesocosm was filled sequentially A to L. Control mesocosms were A, C, E, G, I and K. The phytoplankton bloom was induced in nutrient amended mesocosms B, D, F, H, J and L.

Figure 2. Dissolved inorganic nutrient concentration changes in control (□) and nutrient amended mesocosms (■). Mean value plotted (n = 6) with the error bar representing the standard error.

Figure 3. Changes in abundances of phytoplankton and bacterial cells in the surface microlayer (▲) and subsurface water (■). The surface microlayer was sampled using a mesh screen. The control mesocosm samples have clear symbols and the nutrient amended mesocosm samples have solid symbols. Mean value plotted (n = 6) with the error bar representing the standard error.

Figure 4. Ordination diagram from PCA of bacterial T-RFLP profiles. Samples were collected on day two (red), day five (blue) and day ten (green). Subsurface water (■) was collected using a siphon and the surface microlayer was sampled using two methods: a mesh screen (▲) and polycarbonate membranes (●). The control mesocosm samples have clear symbols and the nutrient amended mesocosm samples have solid symbols.

Figure 5. Bacterial DGGE profiles from day two, day five and day ten. DGGE profiles show each replicate from the subsurface water (SS) and from the surface

microlayer sampled using a mesh screen (MS) and polycarbonate membranes (PC). Beside each DGGE profile is the associated UPGMA dendrogram showing the similarity of the lanes in the DGGE profiles. The arrows show which DGGE bands were excised and sequenced (Table 1).

B.

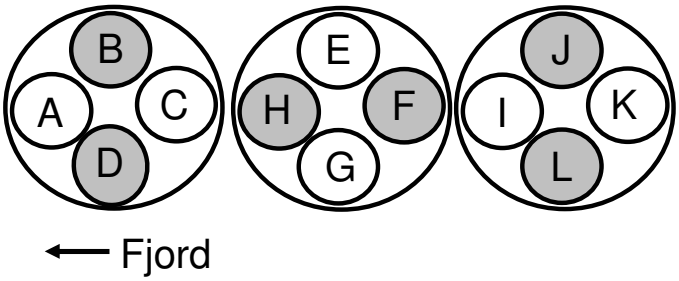

Figure 1.

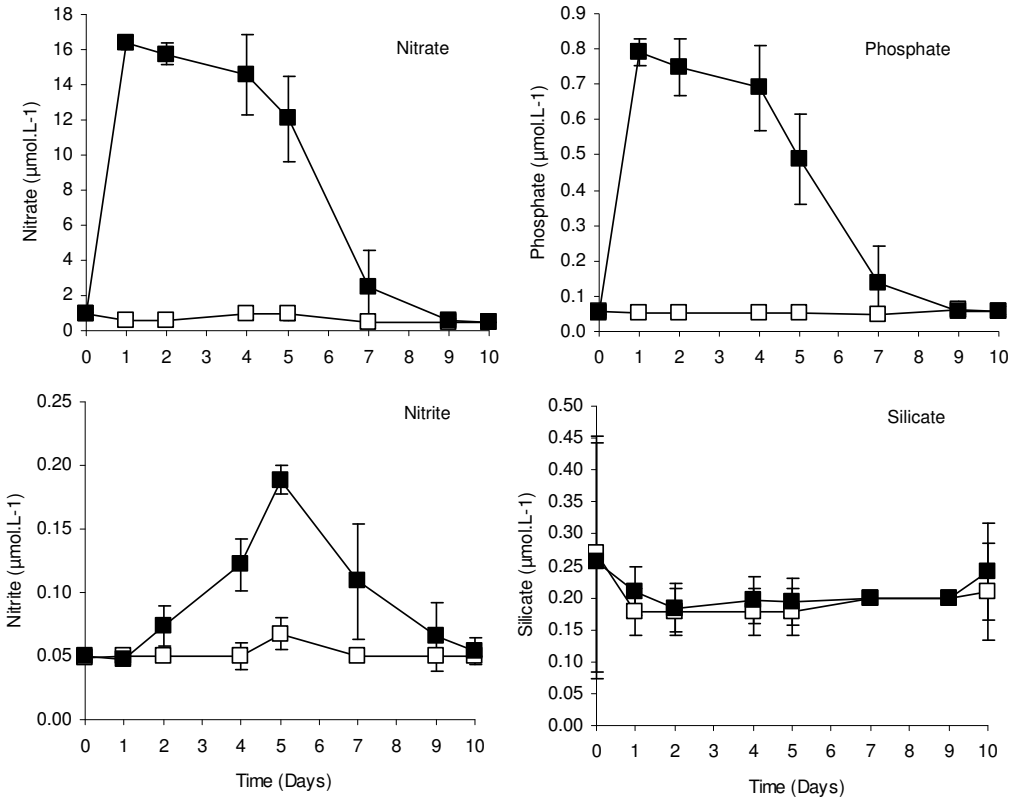

Figure 2.

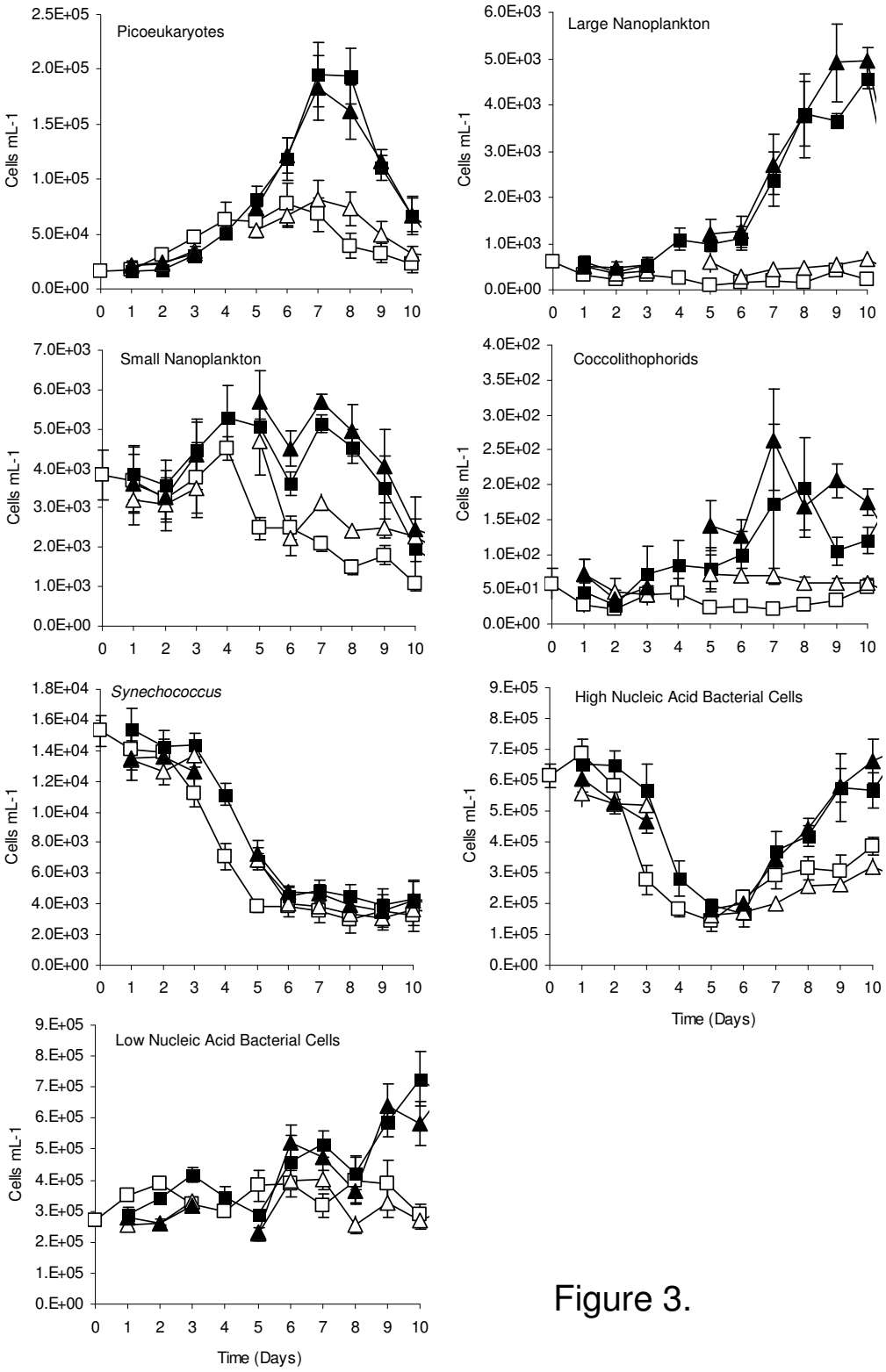

Figure 3.

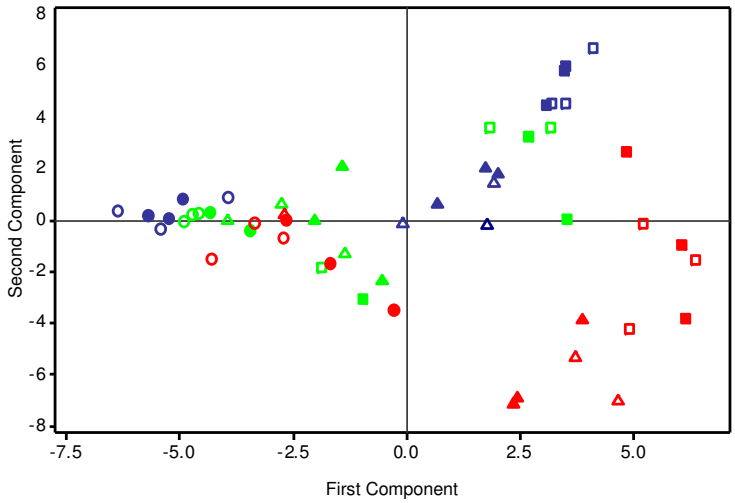

Figure 4.

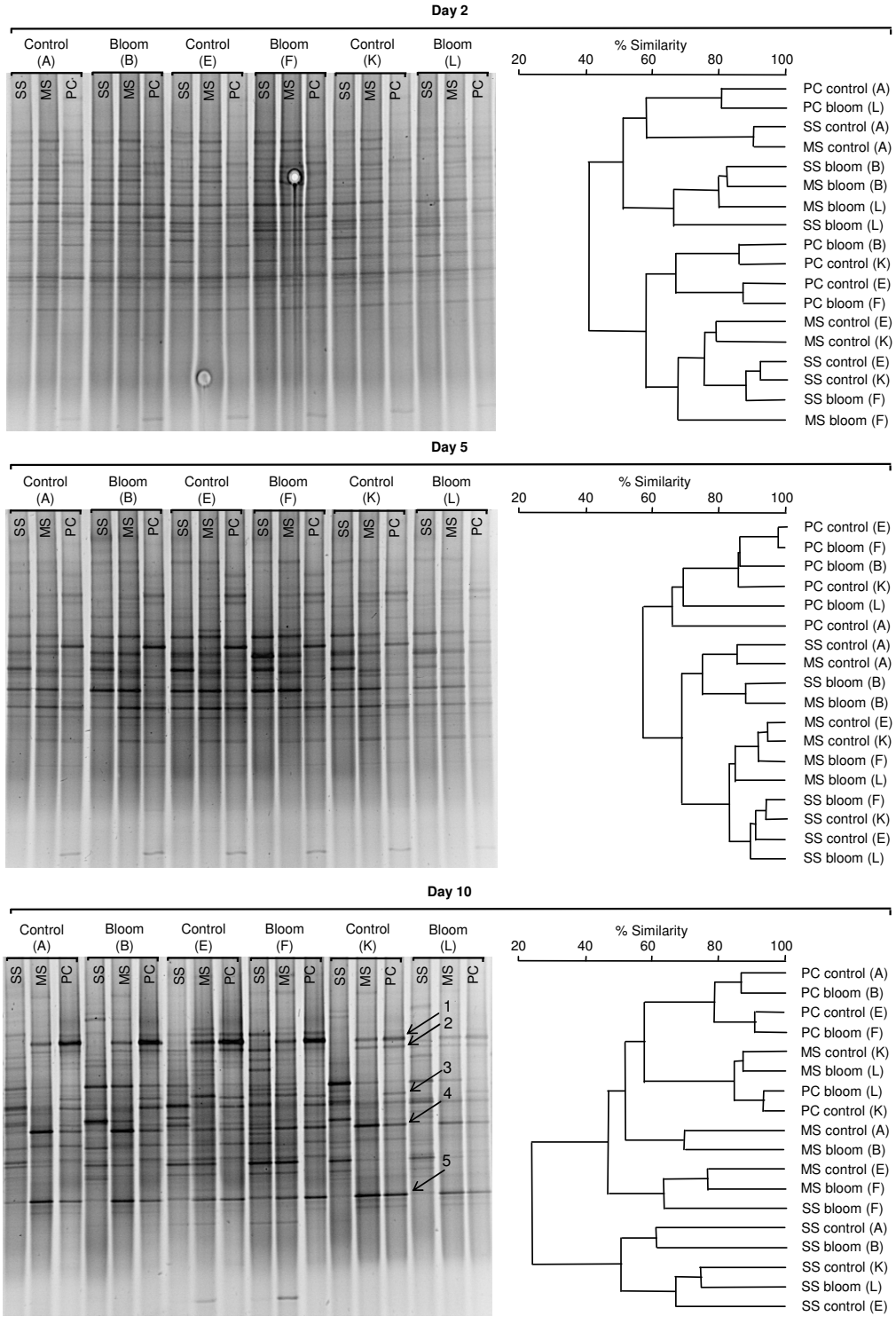

Figure 5.